Single-shot extreme ultraviolet laser imaging of nanostructures with wavelength resolution

Courtney A. Brewer,[1,]* Fernando Brizuela,[1] Przemyslaw Wachulak,[1] Dale H. Martz,[1] Weilun Chao,[2] Erik H. Anderson,[2] David T. Attwood,[2] Alexander V. Vinogradov,[3] Igor A. Artyukov,[3] Alexander G. Ponomareko,[4] Valeriy V. Kondratenko,[4] Mario C. Marconi,[1] Jorge J. Rocca,[1] and Carmen S. Menoni[1]

[1]*National Science Foundation Engineering Research Center for Extreme Ultraviolet Science and Technology, Colorado State University, Fort Collins, Colorado 80523, USA*

[2]*National Science Foundation Engineering Research Center for Extreme Ultraviolet Science and Technology and Center for X-ray Optics, Lawrence Berkeley National Laboratory, Berkeley, California 94720, USA*

[3]*P. N. Lebedev Physical Institute, 53 Leninsky Prospekt, Moscow 119991, Russia*

[4]*National Technical University Kharkov Polytechnic Institute, 21 Frunze Street, Kharkov 61002, Ukraine*

*Corresponding author: brewerca@engr.colostate.edu

We have demonstrated near-wavelength resolution microscopy in the extreme ultraviolet. Images of 50 nm diameter nanotubes were obtained with a single ~ 1 ns duration pulse from a desktop-size 46.9 nm laser. We measured the modulation transfer function of the microscope for three different numerical aperture zone plate objectives, demonstrating that 54 nm half-period structures can be resolved. The combination of near-wavelength spatial resolution and high temporal resolution opens myriad opportunities in imaging, such as the ability to directly investigate dynamics of nanoscale structures. © 2008 Optical Society of America

OCIS codes: 180.7460, 110.7440, 140.7240.

Conventional visible light microscopy, the most convenient method to image small objects, is limited in resolution to ~ 200 nm [1]. A direct approach to overcome this limitation is the use of shorter wavelength extreme ultraviolet (EUV) or soft x-ray (SXR) light [2–11]. The highest spatial resolution achieved to date was obtained at the Advanced Light Source, a third-generation synchrotron, where images with 15 nm half-period spatial resolution were acquired in exposure times of several seconds using 1.52 nm wavelength SXR light [2]. The need for compact and more broadly accessible full-field optical microscopes has motivated the development of microscopes based on high-harmonic light sources [5,6], plasma sources [7], and EUV and SXR lasers [8–11]. However, in all cases the spatial resolution achieved was several times the wavelength and/or required long exposures.

In this Letter we report what is to our knowledge the first EUV microscope that can obtain images with a spatial resolution approaching the wavelength of illumination, in this case $\lambda = 46.9$ nm ($h\nu = 26.4$ eV). Moreover, this microscope can obtain high spatial resolution images with a single laser shot, corresponding to ~ 1 ns temporal resolution, opening the possibility of investigating the dynamics of nanoscale structures. This is possible due to the high brightness of the laser source, the high throughput of the optics, and the ability to tailor the spatial coherence of the laser to reduce coherence effects that can degrade single-shot images. The entire microscope is extremely compact, occupying an area of 0.4 m $\times 2.5$ m. The combination of these attributes results in the demonstration of a high-resolution tool that can rapidly acquire full-field images for practical laboratory use in a broad range of applications.

The microscope is illustrated in Fig. 1. Two spherical Sc–Si multilayer mirrors arranged in a Schwarzschild configuration with 13% throughput condense the light from the output of the laser onto the sample. A freestanding objective zone plate lens projects the image onto a charge-coupled device (CCD) detector with 13.5 μm pixels. The laser beam is created via a highly ionized plasma column that is generated by fast electrical discharge excitation of an Ar-filled capillary [12]. It emits laser pulses with ~ 10 μJ of energy (2.4×10^{12} photons/pulse) and high monochromaticity ($\Delta\lambda/\lambda \approx 5 \times 10^{-5}$), which is ideal for the use of chromatically dependent zone plates. The plasma in the capillary has a convex axisymmetric electron
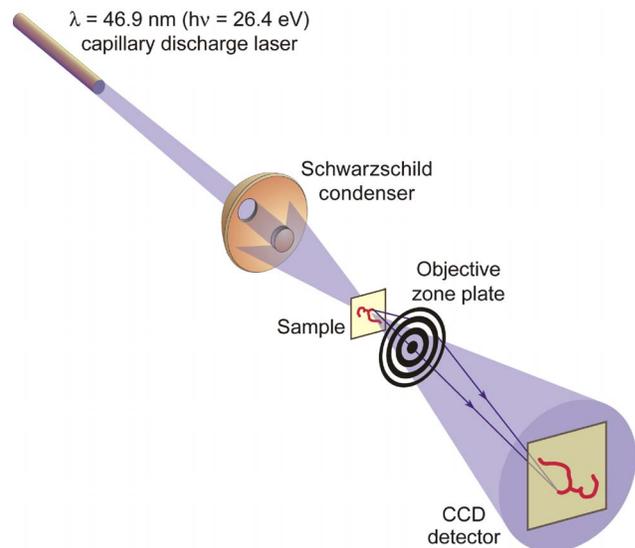

Fig. 1. (Color online) Schematic of the compact 46.9 nm wavelength microscope.

density profile with an on-axis maximum that causes refraction of the amplified light. This provides a mode selection mechanism that filters higher-order modes and reduces the effective transverse source size significantly as the gain medium lengthens. The capillary length of 22 cm selected for these experiments produces optimized, partially coherent pulses for illumination that limit speckle effects that can degrade image quality, while still providing sufficient photon flux for single-shot imaging.

In this work we used three objective zone plates with outer zone widths of $\Delta r = 200$, 124, and 73 nm (NA=0.12, 0.19, and 0.32, respectively). The zone plates were produced by electron-beam lithography on ~100 nm Si_3N_4 membranes [13]. They are freestanding, containing pseudorandom supportive spokes between the zones, to allow a throughput near the full 10% efficiency of the first diffraction order.

The resolving ability of the microscope was evaluated by measuring the modulation transfer function (MTF) for each zone plate objective. Here we define the spatial resolution to be the half-period of a grating for which its image exhibits an intensity modulation of 0.265, derived from the Rayleigh criterion for two imaged point sources [14,15]. To determine the MTF for each objective, we obtained single-shot images of freestanding transmission gratings with spatial half-periods ranging from 300 to 54 nm.

Figures 2(a) and 2(c) are EUV images of two of the smallest half-period gratings, 70 and 54 nm, obtained using the $\Delta r = 73$ nm zone plate. The magnification was 1200×, corresponding to a pixel size of 11 nm at the sample. Scanning electron microscope (SEM) images of portions of the gratings are shown

in the bottom left corners of the EUV images. Figures 2(b) and 2(d) show intensity lineouts for the two images, with average modulation values of 0.83 and 0.33, respectively. Both images satisfy the Rayleigh-like criterion and thus are considered fully resolved. The MTF for each zone plate is shown in Fig. 3. For each image, multiple intensity lineouts were sampled and averaged to obtain the corresponding value and error bar. As expected, for a constant wavelength of illumination, the MTF curve extends to higher spatial frequencies as the NA of the objective increases. For the $\Delta r = 200$, 124, and 73 nm zone plates, near diffraction-limited half-period spatial resolution values of 120, 80, and 54 nm, respectively, were measured. With a spatial resolution of 54 nm, this microscope is to our knowledge the first in the EUV region with the ability to resolve features of dimensions closely approaching the wavelength of illumination.

To illustrate the use of the microscope, we selected an object of dimensions similar to the measured resolution limit of the microscope. We imaged C nanotubes with diameters of ~50 nm, as determined by SEM images, which were deposited onto a ~100 nm thick Si membrane with ~30% transmission at a wavelength of 46.9 nm. Figure 4 is a single-shot image of an entanglement of several C nanotubes, in which features such as nanotube bifurcations are visible.

Although the images presented herein were obtained collecting the transmitted light through the samples, the microscope can be readily reconfigured to acquire images in reflection mode [10]. Furthermore, the ability of this EUV microscope to resolve wavelength-size features with a single laser shot will enable the study of dynamics on nanosecond time
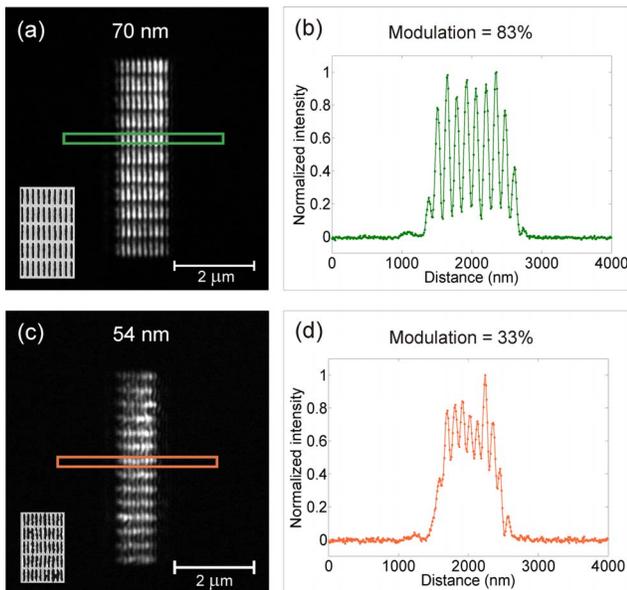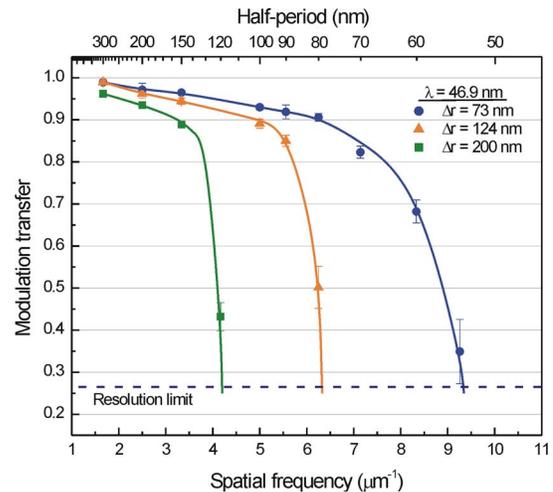

Fig. 2. (Color online) Single-shot EUV images of (a) a 70 nm half-period grating and (b) its corresponding lineout with an 83% intensity modulation, and (c) a 54 nm half-period grating with (d) an intensity lineout showing an average modulation of 33%. The EUV images were acquired using a zone plate objective having an outer zone width of $\Delta r = 73$ nm (NA=0.32). SEM images of portions of the gratings are displayed in the lower corner of the EUV images.

Fig. 3. (Color online) Measured MTFs for objective zone plates with outer zone widths of $\Delta r = 200$, 124, and 73 nm (NA=0.12, 0.19, and 0.32, respectively). The intensity modulation transfer is graphed as a function of the half-period of the grating sample and the spatial frequency, the inverse of the spatial period. The modulation transfer values were obtained by averaging multiple intensity lineouts within an image, and the curves were added to guide the eye. For the $\Delta r = 200$, 124, and 73 nm zone plates, Rayleigh-like resolution values of 120, 80, and 54 nm, respectively, were measured.
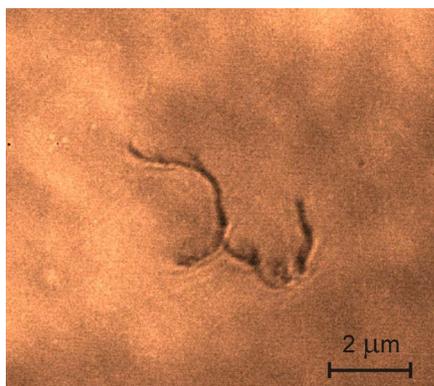
Fig. 4. (Color online) Single-shot image of an entanglement of 50 nm diameter carbon nanotubes. This image was obtained using the $\Delta r = 73$ nm objective lens and a wavelength of 46.9 nm. Features such as nanotube bifurcations are visible.

scales. Based on these results, we anticipate that recently developed high brightness tabletop lasers at wavelengths near 13 nm [16] will enable the acquisition of images with spatial resolution approaching 15 nm and picosecond temporal resolution. At these shorter wavelengths, microscopes will be particularly advantageous as mask inspection tools for the EUV lithography industry. Moreover, these practical compact EUV and SXR laser-based full-field microscopes will allow the study of ultrafast processes with nanometer-scale resolution, becoming an enabling tool for a wide range of nanoscience and nanotechnology applications.

References

1. Y. Garini, B. J. Vermolen, and I. T. Young, Curr. Opin. Biotechnol. **16**, 3 (2005).
2. W. Chao, B. D. Harteneck, J. A. Liddle, E. H. Anderson, and D. T. Attwood, Nature **435**, 1210 (2005).
3. D. S. DiCicco, D. Kim, R. Rosser, and S. Suckewer, Opt. Lett. **17**, 157 (1992).
4. L. B. Da Silva, J. E. Trebes, R. Balhorn, S. Mrowka, E. Anderson, D. T. Attwood, T. W. J. Barbee, J. Brase, M. Corzett, J. Gray, J. A. Koch, C. Lee, D. Kern, R. A. London, B. J. MacGowan, D. L. Matthews, and G. Stone, Science **258**, 269 (1992).
5. M. Wieland, C. Spielmann, U. Kleineberg, T. Westerwalbesloh, U. Heinzmann, and T. Wilhein, Ultramicroscopy **102**, 93 (2005).
6. R. L. Sandberg, A. Paul, D. A. Raymondson, S. Hädrich, D. M. Gaudiosi, J. Holtsnider, R. I. Tobey, O. Cohen, M. M. Murnane, H. C. Kapteyn, C. Song, J. Miao, Y. Liu, and F. Salmassi, Phys. Rev. Lett. **99**, 098103 (2007).
7. P. A. C. Takman, H. Stollberg, G. A. Johansson, A. Holmberg, M. Lindblom, and H. M. Hertz, J. Microsc. **226**, 175 (2007).
8. M. Kishimoto, M. Tanaka, R. Tai, K. Sukegawa, M. Kado, N. Hasegawa, H. Tang, T. Kawachi, P. Lu, K. Nagashima, H. Daido, Y. Kato, K. Nagai, and H. Takenaka, J. Phys. IV **104**, 141 (2003).
9. G. Vaschenko, F. Brizuela, C. Brewer, M. Grisham, H. Mancini, C. S. Menoni, M. C. Marconi, J. J. Rocca, W. Chao, J. A. Liddle, E. H. Anderson, D. T. Attwood, A. V. Vinogradov, I. A. Artioukov, Y. P. Pershyn, and V. V. Kondratenko, Opt. Lett. **30**, 2095 (2005).
10. F. Brizuela, G. Vaschenko, C. Brewer, M. Grisham, C. S. Menoni, M. C. Marconi, J. J. Rocca, W. Chao, J. A. Liddle, E. H. Anderson, D. T. Attwood, A. V. Vinogradov, I. A. Artioukov, Y. P. Pershyn, and V. V. Kondratenko, Opt. Express **13**, 3983 (2005).
11. G. Vaschenko, C. Brewer, E. Brizuela, Y. Wang, M. A. Larotonda, B. M. Luther, M. C. Marconi, J. J. Rocca, and C. S. Menoni, Opt. Lett. **31**, 1214 (2006).
12. S. Heinbuch, M. Grisham, D. Martz, and J. J. Rocca, Opt. Express **13**, 4050 (2005).
13. E. H. Anderson, IEEE J. Quantum Electron. **42**, 27 (2006).
14. D. T. Attwood, *Soft X-Rays and Extreme Ultraviolet Radiation: Principles and Applications* (Cambridge U. Press, 2000).
15. J. M. Heck, D. T. Attwood, W. Meyer-Ilse, and E. H. Anderson, J. X-Ray Sci. Technol. **8**, 95 (1998).
16. J. J. Rocca, Y. Wang, M. A. Larotonda, B. M. Luther, M. Berrill, and D. Alessi, Opt. Lett. **30**, 2581 (2005).